

Pulsing and Non-Pulsing ULXs: the Iceberg Emerges

Andrew King^{1,2,3,4} & Jean-Pierre Lasota^{4,5}

¹ *Theoretical Astrophysics Group, School of Physics & Astronomy, University of Leicester, Leicester LE1 7RH, UK*

² *Astronomical Institute Anton Pannekoek, University of Amsterdam, Science Park 904, 1098 XH Amsterdam, Netherlands*

³ *Leiden Observatory, Leiden University, Niels Bohrweg 2, NL-2333 CA Leiden, Netherlands*

⁴ *Institut d'Astrophysique de Paris, CNRS et Sorbonne Université, UMR 7095, 98bis Bd Arago, 75014 Paris, France*

⁵ *Nicolaus Copernicus Astronomical Center, Polish Academy of Sciences, ul. Bartycka 18, 00-716 Warsaw, Poland*

20 February 2024

ABSTRACT

We show that ultraluminous X-ray sources (ULXs) with coherent X-ray pulsing (PULXs) probably have neutron-star spin axes significantly misaligned from their central accretion discs. Scattering in the funnels collimating their emission and producing their apparent super-Eddington luminosities is the most likely origin of the observed correlation between pulse fraction and X-ray photon energy. Pulsing is suppressed in systems with the neutron-star spin closely aligned to the inner disc, explaining why some ULXs show cyclotron features indicating strong magnetic fields, but do not pulse. We suggest that alignment (or conceivably, field suppression through accretion) generally occurs within a fairly short fraction of the ULX lifetime, so that most neutron-star ULXs become unpulsed. As a result we further suggest that almost all ULXs actually have neutron-star accretors, rather than black holes or white dwarfs, reflecting their progenitor high-mass X-ray binary and supersoft X-ray source populations.

Key words: accretion, accretion discs – binaries: close – X-rays: binaries – black hole physics – neutron stars – pulsars: general

1 INTRODUCTION

Ultraluminous X-ray sources (ULXs) are objects with apparent (i.e. assumed isotropic) luminosities $L_{\text{app}} \gtrsim 10^{39} \text{ erg s}^{-1}$, exceeding the usual Eddington value for stellar-mass black holes, but which do not contain supermassive black holes.

Their discovery around the turn of the century prompted initial suggestions that they contained black holes with ‘intermediate’ masses, i.e. above the then accepted maximum value $\sim 10 M_{\odot}$ for black holes produced by stellar evolution, but below supermassive (e.g. Colbert & Mushotzky 1999).

But it is now widely accepted (cf Kaaret, Feng & Roberts 2017) that most if not all ULXs are stellar-mass binary systems, as first suggested by King et al. (2001). The distinctive features of ULXs probably result from mass transfer rates which would produce luminosities significantly above Eddington if they could be entirely accreted. Systems like this are the natural outcome of high-mass X-ray binary (HMXB) evolution, where the accretor is a neutron star (or in a few cases a stellar-mass black hole) accreting from a more massive and largely radiative companion. Once the companion star’s nuclear evolution expands it to the point of filling its Roche lobe, it transfers mass to the compact star (neutron star or black hole). Because

it puts mass further from the binary mass centre this process shrinks the binary, increasing the transfer rate. However runaway mass transfer is avoided, as the largely radiative donor star (of mass M_2) cannot expand faster than given by its thermal timescale t_{KH} (cf King & Ritter 1999; King & Begelman 1999; King, Taam & Begelman 2000, ; the basic result goes back to Kippenhahn & Weigert (1967); Kippenhahn, Kohl & Weigert (1967)) giving transfer rates $\dot{M} \sim M_2/t_{\text{KH}} \sim 10^{-7} - 10^{-5} M_{\odot} \text{ yr}^{-1}$ or even more, well above the Eddington rate $\dot{M}_{\text{Edd}} = L_{\text{Edd}}/\eta c^2$ needed to produce L_{Edd} , where $\eta \sim 0.1$ the accretion efficiency. Supersoft X-ray sources probably have similar thermal-timescale mass transfer on to white dwarfs, and in some extreme cases ($\dot{M} \gtrsim 10^{-5} M_{\odot} \text{ yr}^{-1}$) may produce ULXs with white-dwarf accretors (King et al., 2001; Fabbiano et al., 2003). Several ULXs have Be-type companion stars. Here super-Eddington accretion is not a result of thermal-timescale mass transfer, but instead occurs only episodically because the Be-star disc undergoes Kozai–Lidov cycles (Martin et al. 2014).

Recently, wind Roche-lobe overflow has been proposed as a possible mass-transfer mechanism in ULXs (El Mellah, Sundqvist & Keppens 2019; Heida, et al. 2019a,b). This automatically occurs if the companion’s stellar wind has a velocity smaller than the orbital velocities of the binary components. But despite the claims in El Mellah, Sundqvist &

Keppens (2019), there is no need to invoke this process to avoid runaway (‘unstable’) mass transfer once the stellar photosphere fills the Roche lobe, since this is limited to the thermal-timescale rate discussed above.

In all cases, the excess transferred mass is not accreted but ejected, as envisaged by Shakura & Sunyaev (1973). This explains the survival of the neutron star in Cyg X-2 with only modest mass gain after strongly super-Eddington accretion (King & Ritter, 1999). The excess is largely driven away from the accretor at a characteristic disc ‘spherization’ radius

$$R_{\text{sph}} \simeq \frac{27}{4} \dot{m} R_g \quad (1)$$

as a quasispherical wind (of velocity $\sim 0.1c$, King & Pounds, 2003), which leaves narrow open channels around the accretion disc axis. (Here $\dot{m} = \dot{M}/\dot{M}_{\text{Edd}}$ is the accretor’s Eddington factor, \dot{M} is the mass transfer rate from the companion, and $R_g = GM/c^2$ is the gravitational radius.) The collimating structure of this wind causes most emitted radiation to escape along the narrow channels around the accretion disc axis and makes the true emission pattern strongly anisotropic. When viewed along these directions the assumption of isotropic emission implies a much larger apparent luminosity

$$L_{\text{app}} = L_{\text{sph}} \simeq \frac{1}{b} L \quad (2)$$

than the true value $L \simeq L_{\text{Edd}}(1 + \ln \dot{m})$. Here $b < 1$ is a beaming factor, later found to be approximated by

$$b \simeq \frac{73}{\dot{m}^2} \quad (3)$$

(King 2009). This particular form assumed accretion on to a black hole, and one might ask if the formula should change in other cases. But within R_{sph} , the accretion rate decreases as $\dot{M}(R) = \dot{M}(R/R_{\text{sph}})$ as gas is progressively expelled. This means that the vast bulk of the outflow causing the collimation (‘beaming’) is expelled near R_{sph} , quite independently of what happens at smaller radii. In particular we shall use this form to describe accretion in PULXs, where the disc is disrupted by the neutron-star magnetic field at a radius $R_M < R_{\text{sph}}$, and gas inflow is along fieldlines for $R < R_M$. We note that our application of this picture to PULXs leads self-consistently to values of R_M smaller than R_{sph} and magnetic fields $\sim 10^{11} - 10^{13}$ G (King, Lasota & Kluźniak 2017).

In suggesting this picture King et al. (2001) noted its implication that ULX luminosities alone do not directly tell us the nature of the accretor, only that its mass must be smaller than the value found by assuming $L_{\text{sph}} = L_{\text{Edd}}$. Accordingly they pointed out that not all ULXs had to contain black holes, and predicted that some might instead contain neutron stars or even white dwarfs, for mass transfer rates $\gtrsim 10^{-8}$ or $10^{-5} M_{\odot} \text{ yr}^{-1}$ respectively. (Fabbiano et al. 2003, identified a possible white dwarf ULX on the basis of its unusually soft emission.) In the last few years observations have revealed at least 10 of the predicted neutron-star ULX systems, beginning with ULX M82 X-2 (Bachetti et al. 2014), which has a coherent X-ray periodicity $P = 1.37$ s, naturally interpreted as the spin period of an accreting magnetic neutron star (see Table A1). Several of these systems have Be-type companion stars (see also Table 1).

There were initial suggestions that these pulsing ULXs (PULXs) might somehow evade the Eddington limit by having unusually strong (magnetar-like: $B > 10^{13}$ G) magnetic fields which reduced the electron-scattering cross-section (see e.g., Ekşi et al. 2015; Mushtukov, et al. 2015), but these are contradicted by the 10^{12} G fields found from cyclotron lines seen in NGX300 ULX-1 (Walton et al. 2018b) and in the non-pulsing ULX-8 in M51 (Brightman et al. 2018; Middleton et al. 2019).

Mushtukov et al. (2019) also argue that strong outflows observed in PULXs imply normal pulsar-strength magnetic fields in these objects. These authors point out that the detection of a strong outflow from a PULX is evidence for a relatively weak dipole neutron-star magnetic field. They also note that an outflow was recently discovered from ULX-1 in NGC 300 (Kosec, et al. 2018), for which Carpano et al. (2018) deduced a magnetic field of $B \sim 10^{12}$ G. Our model (see below) predicts $B = 1.2 \times 10^{12}$ G for this source (see King & Lasota 2019, and Table 1).

King & Lasota (2019, hereafter KL19) noted that the high pulse spinup rates $\dot{\nu}$ observed in the first discovered PULXs (Kluźniak & Lasota 2015; King & Lasota 2016; King, Lasota & Kluźniak 2017) are a distinctive feature of all pulsing ULXs: they are systematically higher than in all other pulsing X-ray binaries (KL19, Fig. 1). Adopting equations (2) and (3), and using standard theory for accretion-driven spinup of magnetic neutron stars, KL19 found the striking result that for all observed PULXs, the magnetospheric (Alfvén) radius R_M , where the accretion flow begins to follow fieldlines, is only slightly smaller than the spherization radius, i.e.

$$R_M \lesssim R_{\text{sph}}. \quad (4)$$

It is easy to interpret this relation as a necessary condition for a significant pulse fraction to be observable. But it is important to note that it was not assumed in advance of the calculation: this necessary condition for observable pulsing results simply from applying the theory of Shakura & Sunyaev (1973) for super-Eddington mass supply to the case of a magnetic accretor.

A second significant result of KL19’s analysis is that all the magnetic fields B deduced for observed PULXs lie in the usual range $10^{11} - 10^{13}$ G for all other pulsing X-ray sources (Table 2 in KL19 and Table 1 in the present paper). There is no need to invoke a new population of neutron stars with unusually strong magnetic fields to explain the PULX population.

This agrees with the observational facts that the measured fields in ULXs are all in the normal X-ray source range (see above), and that no magnetar has yet been found to be a member of a binary system. In addition there appears to be no easy way of forming such a system (see, e.g., KL19). For completeness we give here in Table 1 an updated version of Table 2 of KL19, adding one new source (M51 ULX7) and giving the magnetic field values B (rather than the magnetic moments μ), together with the deduced beaming factors b .

Suggestions that some of the excess accreting matter might be ‘advected’ on to the compact accretor’s surface (Chashkina, et al. 2019) are not appropriate for neutron stars – see e.g. the simulations by Takahashi, Mineshige & Ohsuga (2018)) where the advection on to the surface is “very small” in a nonmagnetic case, and by Kawashima, et

Table 1. Derived properties of PULXs (updated Table 2 from King & Lasota (2019); see Table A1 for observational data.)

Name	\dot{m}_0	b	$B q^{7/4} m_1^{-1/2} I_{45}^{-3/2} R_6^3$ [G]	$R_{\text{sph}} m_1^{-1}$ [cm]	$R_M m_1^{-1/3} I_{45}^{-2/3}$ [cm]	$P_{\text{eq}} q^{-7/6} m_1^{1/3}$ [s]	t_{eq} [yr] ¹
M82 ULX2	36	0.06	9.0×10^{10}	3.6×10^7	1.0×10^7	0.02	15600
NGC 7793 P13	20	0.05	2.5×10^{11}	2.1×10^7	1.6×10^7	0.09	1386
NGC5907 ULX1	91	0.009	2.1×10^{13}	9.1×10^7	1.1×10^8	1.86	0
NGC300 ULX1	20	0.05	$1.2 \times 10^{12\heartsuit}$	2.1×10^7	3.2×10^7	0.19	297
M51 ULX7 ^a	28	0.09	1.9×10^{11}	2.9×10^7	2.0×10^7	0.08	1337
M51 ULX7 ^b	28	0.09	6.9×10^9	2.9×10^7	4.6×10^6	0.01	$\sim 10^5$
SMC X-3 ^{Be}	18	0.23	2.3×10^{10}	1.8×10^7	7.1×10^6	0.006	76621
NGC 2403 ULX ^{Be}	11	0.60	5.6×10^{11}	1.1×10^7	2.3×10^7	0.16	578
Swift J0243.6+6124 ^{Be}	14	0.37	1.6×10^{11}	1.4×10^7	1.7×10^7	0.07	2047
NGC 1313 ULX ^{Be}	14	0.37		2.8×10^7			
M51 ULX8	16	0.29	$\sim 3 \times 10^{11}\clubsuit$	1.6×10^7	$2.7 \times 10^7\spadesuit$	non-pulsing	

– Systems with ^{Be} superscript have Be-star companions.

¹ - calculated using the value of $P_{\text{eq}} q^{-7/6} m_1^{1/3}$ from the previous column.

[♥] – confirmed by observations Walton et al. (2018b).

[♣] – from observations (Brightman et al. 2018; Middleton et al. 2019).

[♠] – for a $\sim 10^{12}$ G magnetic field.

^a – for $\dot{\nu} = 2.8 \times 10^{-10}$; ^b – for $\dot{\nu} = 3.1 \times 10^{-11}$ (Vasilopoulos et al. 2019).

al. (2016); Kawashima & Ohsuga (2020), Inoue, Ohsuga & Kawashima (2020) who show that emission from the neutron star surface at the bottom of the accretion column is negligible. It is well established that the presence or absence of a critical (sonic) point above the accretor surface completely changes the nature of the accretion flow (Abramowicz, et al. 2010; Lipunova 1999).

The results of KL19 offer a tightly self-consistent picture of accretion in neutron-star ULXs, which applies to stellar-mass black-hole accretors also. A super-Eddington mass supply ($\dot{M} > \dot{M}_{\text{Edd}}$) to a magnetic neutron star is partially ejected in the way proposed by Shakura & Sunyaev (1973), giving natural explanations for the distinctive observed features of ULXs and PULXs.

Given this agreement, one can attempt a more detailed analysis. PULXs have significant pulse fractions, up to $\sim 50\%$ (Kaaret, Feng & Roberts 2017), and this is sometimes seen as difficult to make compatible with significant beaming. This paper discusses this systematically. We will see that the conditions needed for large pulse fractions strongly constrain the ULX population.

2 PULSING

X-ray pulse light curve for PULXs are essentially ‘sinusoidal’, i.e. without obvious eclipses, and continuously modulated. Mushtukov et al. (2017, 2019) drew the conclusion that the X-ray emission region must in general have an area comparable with that of the neutron star, as otherwise there would be systems in which this region would either be permanently in view, or periodically occulted. The resulting

largely unmodulated emission, or eclipses, would conflict with the observed sinusoidal character, and Mushtukov et al. (2017, 2019) suggested that the X-rays come from an optically thick envelope defined by the accretion flow over the neutron-star magnetosphere. This is physically reasonable, as the accretion along fieldlines is a bending hypersonic flow, which must therefore shock (King, Lasota & Kluźniak 2017, KL19).

But the problem is subtle. The absence of observed eclipses is much stronger evidence for extended emission regions than the lack of unmodulated emission. Most ULXs do not show pulsing, so it is possible that there are a significant number of magnetic neutron-star accretors amongst them, changing the inferred low probability of unmodulated emission. Support for this view comes from the significant magnetic field inferred from the cyclotron line detected in M51 ULX-8 (Brightman et al. 2018; Middleton et al. 2019). We will see that if the X-rays are beamed, both sinusoidal and unmodulated emission are quite possible for ULXs where the accretor is a neutron star with a normal magnetic field.

Mathematically, the pulsed light-curve problem is identical to that presented by the hard X-ray light curves of intermediate polars, which are close binaries where a magnetic white dwarf with a spin period of a few minutes accretes from a companion in a close orbit of a few hours. Here also the light curves are ‘sinusoidal’, and King & Shaviv (1984, hereafter KS84) drew the same conclusion as Mushtukov et al. (2017, 2019), i.e. that the hard X-ray emission area occupies a large fraction of the white dwarf surface. As there is no evidence for unmodulated intermediate polar systems, this conclusion is not subject to the same possible caveat as mentioned above for ULX neutron-star accretors. To discuss

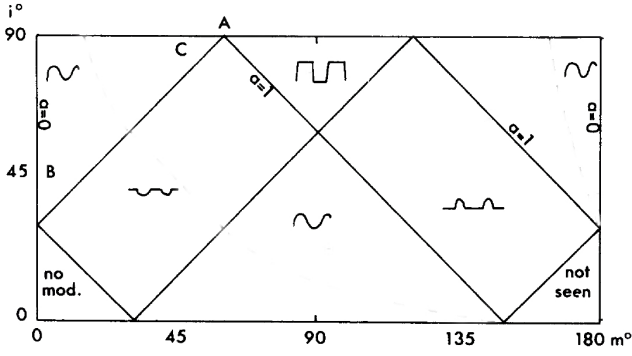


Figure 1. The shapes of X-ray light-curves as functions of angles i (observer inclination) and m (magnetic colatitude) for an accreting, spinning magnetic neutron star with polecap fraction 0.25, adapted from KS84. The predicted spin light-curve shapes are indicated in each case by an obvious shorthand. Observed PULX light curves are continuously modulated (‘sinusoidal’), but there may be a large population of magnetic neutron star ULXs which show *no* spin modulation at all. We suggest that observed PULXs are likely to lie in the region $i \sim 45 - 90^\circ$ and $m \sim 0 - 45^\circ$, where the magnetic axis is strongly misaligned from the spin axis. Alignment of the two axes probably occurs in a timescale rather shorter than the ULX lifetime, so that a majority of ULXs may contain magnetic neutron stars, but not show pulsing.

these systems we use the analysis of KS84, which classifies pulse light curves as functions of the colatitude angle m of the magnetic field wrt the spin axis of the emitting star and the observer inclination i wrt the same axis (for intermediate polars this is identical with the orbital and disc axes, but this is not true for neutron-star ULXs – see the discussion below).

Fig 3 of KS84 shows that the lack of eclipses implies large-area emission regions. Figure 1, based on Fig. 4 in KS84, shows that sinusoidal pulse light-curves can originate from a single ‘upper’ polecap ($m < 90^\circ$) alone if

$$i \sim 45 - 90^\circ \text{ and } m \sim 0 - 45^\circ \quad (5)$$

or

$$i \sim 0 - 45^\circ \text{ and } m \sim 45 - 90^\circ. \quad (6)$$

(Clearly the incidence of ‘sinusoidal’ light curves is increased further if instead of a single polecap, a pair of polecaps [$m > 90^\circ$ as well as $m < 90^\circ$] with different properties are observable at certain spin phases.) The first case (Eq. 5) corresponds to a spin axis strongly misaligned from the central disc axis at the spherization radius (Fig. 2, left), whereas these two axes are closer to alignment in the second case of Eq. 6 (Fig. 2, right).

Both cases are physically possible. The supernova explosion producing the neutron star is known from observation (see e.g., Willems, Kalogera & Henninger 2004) to be sufficiently asymmetric to leave it in general with an initial spin axis strongly misaligned from the central disc axis. But two processes try to align these axes. The first possibility is warping of the central disc into the neutron-star spin plane through differential torques (both magnetic and precessional), and the second is direct accretion of angular

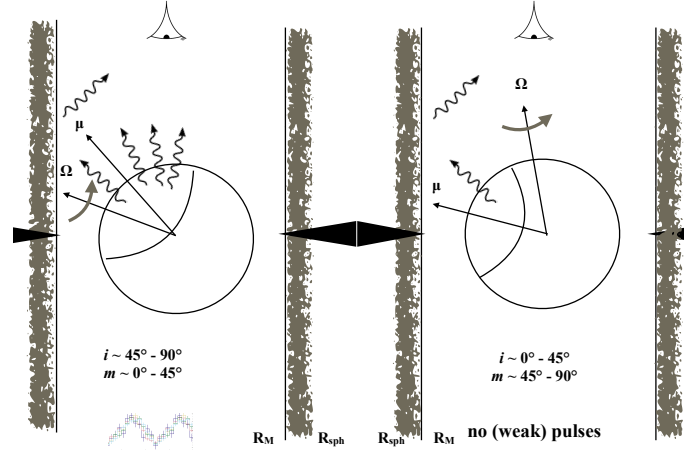


Figure 2. Effect of spin orientation on pulsing. Left: the neutron-star spin and the accretion disc beaming axes are strongly misaligned, so that a significant part of the pulsed emission can escape without scattering. This gives a large pulse fraction. Right: the neutron-star spin and central disc axes are substantially aligned, so that much of the primary X-ray emission is scattered by the walls of the beaming ‘funnel’ before escaping. The pulse fraction is reduced

momentum (characterized by R_M) from an unwarped disc lying in the binary orbital plane. The latter seems more likely, as any interruption in the accretion flow means that disc warping has to ‘start again’. Neither process seems likely to be very efficient in the Be-star PULXs, where accretion is barely super-Eddington and confined to short transient episodes.

The outcomes of the two spin orientations are very different.

- If there is strong misalignment of the spin and beaming axes, a significant part of the pulsed emission can escape without scattering, giving a large pulse fraction (Fig. 2, left). This must be maximal at the highest X-ray energies, as scattering makes the X-rays both softer and less pulsed. This correlation of pulse fraction and X-ray energy is well known for observed PULXs (Kaaret, Feng & Roberts 2017).

- If instead there is substantial alignment of the spin and central disc axes, much of the primary X-ray emission is scattered by the walls of the beaming ‘funnel’ before escaping (Fig. 2, right). Since the light-travel time across the funnel is usually comparable with the pulse duration, the pulse amplitude can be severely reduced. The pulse fraction can of course also be reduced or entirely removed if enough matter accretes to weaken the neutron-star magnetic field. This presumably happened in the case of Cyg X-2, which is a survivor of a phase of strongly super-Eddington accretion (King & Ritter 1999). Here the neutron star is not noticeably magnetic, and has probably gained a few $\times 0.1 M_\odot$ during the super-Eddington phase.

These outcomes appear to agree well with observations of ULXs. Very few ULXs show pulsing. But if most ULXs descend either from HMXBs once the companion star fills its Roche lobe, or from Be-star HMXBs, two lines of argument suggest that the vast (unpulsed) majority of ULXs

must contain neutron stars. First, almost all HMXBs contain neutron stars rather than black holes. Second, as remarked by King (2009) and King & Lasota (2016), neutron-star systems are more super-Eddington and so more beamed than black-hole systems with the same mass-transfer rate, and so have *higher* apparent ULX luminosities. In addition, there is at least one system whose spectrum shows a cyclotron feature corresponding to a pulsar-strength magnetic field (Middleton et al. 2019), but which does not show pulsing, strongly suggesting that it is an aligned accretor.

The fact that the vast majority of ULXs do not pulse, despite containing neutron stars, then implies that alignment of spin and central disc axes is rapid, and possibly that field suppression through accretion occurs also. As expected, Be-star systems are prominent among the PULXs since accretion is relatively weak and transient.

3 CONCLUSIONS

We have shown that PULXs probably have spin axes significantly misaligned from their accretion discs. This geometry naturally reproduces the observed correlation between pulse fraction and X-ray photon energy. If alignment occurs, pulsing is significantly suppressed, explaining the presence of unpulsed ULXs with cyclotron features indicating strong magnetic fields.

We suggest that the timescale for spin alignment (or field suppression by accretion) is short compared with the ULX lifetime, and so that most observed (unpulsed) ULXs contain neutron star accretors, either with spin and central disc accretion closely aligned, or with their initial magnetic fields suppressed by accretion. This is expected if they descend from HMXBs as the companion star fills its Roche lobe. Further searches for cyclotron features in unpulsed ULXs offer a possible check of these ideas.

When first recognised as a class, ULXs were widely assumed to contain black holes of masses $\gtrsim 100 - 10^4 M_\odot$. The suggestion here that the great majority actually instead have neutron-star accretors, with only a few black holes and white dwarfs, is a significant shift of the paradigm (King & Lasota 2016; King, Lasota & Kluźniak 2017, see also Mushukov, et al. (2015)). We suggest that unpulsed ULXs are the ‘iceberg’ envisaged in the latter paper, and PULXs just the tip of it.

ACKNOWLEDGMENTS

We thank the referee for pointing out relevant references and helping to tighten our arguments. ARK gratefully acknowledges support from the Institut d’Astrophysique de Paris. JPL thanks the Nella and Leon Benoziyo Center for Astrophysics of the Weizmann Institute for hospitality and its members, in particular Boaz Katz, for stimulating discussions. This research was supported by the Polish NCN grant No. 2015/19/B/ ST9/01099. JPL acknowledges support from the French Space Agency CNES.

REFERENCES

- Abramowicz M. A., Jaroszyński M., Kato S., Lasota J.-P., Różańska A., Sądowski A., 2010, *A&A*, 521, A15
- Bachetti M., et al., 2014, *Nature*, 514, 202
- Brightman M., et al., 2018, *NatAs*, 2, 312
- Carpano, S., Haberl, F., Maitra, C., & Vasilopoulos, G. 2018, *MNRAS*, 476, L45
- Chashkina A., Lipunova G., Abolmasov P., Poutanen J., 2019, *A&A*, 626, A18
- Colbert E. J. M., Mushotzky R. F., 1999, *ApJ*, 519, 89
- Doroshenko V., Tsygankov S., Santangelo A., 2018, *A&A*, 613, A19
- Eksi, K. Y., Andaç, İ. C., Çıkıntoğlu, S., et al. 2015, *MNRAS*, 448, L40
- El Mellah I., Sundqvist J. O., Keppens R., 2019, *A&A*, 622, L3
- Fabbiano G., King A. R., Zezas A., Ponman T. J., Rots A., Schweizer F., 2003, *ApJ*, 591, 843
- Fürst F., et al., 2016, *ApJ*, 831, L14
- Fürst F., et al., 2018, *A&A*, 616, A186
- Heida M., Harrison F. A., Brightman M., Fürst F., Stern D., Walton D. J., 2019, *ApJ*, 871, 231
- Heida M., et al., 2019, *ApJL*, 883, L34
- Inoue A., Ohsuga K., Kawashima T., 2020, *PASJ*.tmp, doi:10.1093/pasj/psaa010
- Israel G. L., et al., 2017, *MNRAS*, 466, 48
- Israel G. L., et al., 2017, *Sci*, 355, 817
- Kaaret P., Feng H., Roberts T. P., 2017, *ARA&A*, 55, 303
- Kawashima T., Mineshige S., Ohsuga K., Ogawa T., 2016, *PASJ*, 68, 83
- Kawashima T., Ohsuga K., 2020, *PASJ*, 72, 15
- King A. R., 2009, *MNRAS*, 393, L41
- King A. R., Begelman M. C., 1999, *ApJL*, 519, L169
- King A., Lasota J.-P., 2016, *MNRAS*, 458, L10
- King A., Lasota J.-P., 2019, *MNRAS*, 485, 3588 [KL19]
- King A., Lasota J.-P., Kluźniak W., 2017, *MNRAS*, 468, L59
- King A. R., Davies M. B., Ward M. J., Fabbiano G., Elvis M., 2001, *ApJ*, 552, L109
- King A. R., Ritter H., 1999, *MNRAS*, 309, 253
- King A. R., Shaviv G., 1984, *MNRAS*, 211, 883 [KS84]
- King A. R., Taam R. E., Begelman M. C., 2000, *ApJL*, 530, L25
- Kippenhahn R., Weigert A., 1967, *ZA*, 65, 251
- Kippenhahn R., Kohl K., Weigert A., 1967, *ZA*, 66, 58
- Kluźniak W., Lasota J.-P., 2015, *MNRAS*, 448, L43
- Kosec P., et al., 2018, *MNRAS*, 479, 3978
- Lipunova G. V., 1999, *AstL*, 25, 508
- Martin R. G., Nixon C., Armitage P. J., Lubow S. H., Price D. J., 2014, *ApJ*, 790, L34
- Middleton M., Brightman M., Pintore F., Bachetti M., Fabian A., Fuerst F., Walton D., 2019, *MNRAS*, 468, 2
- Motch C., Pakull M. W., Soria R., Grisé F., Pietrzyński G., 2014, *Nature*, 514, 198
- Mushtukov A. A., Suleimanov V. F., Tsygankov S. S., Poutanen J., 2015, *MNRAS*, 454, 2539
- Mushtukov A. A., Suleimanov V. F., Tsygankov S. S., Ingram A., 2017, *MNRAS*, 467, 1202
- Mushtukov A. A., Ingram A., Middleton M., Nagirner D. I., van der Klis M., 2019, *MNRAS*, 484, 687
- Rodríguez Castillo G. A., et al., 2019, *arXiv*,

- arXiv:1906.04791
 Shakura N. I., Sunyaev R. A., 1973, *A&A*, 24, 337
 Takahashi H. R., Mineshige S., Ohsuga K., 2018, *ApJ*, 853, 45
 Townsend L. J., Kennea J. A., Coe M. J., McBride V. A., Buckley D. A. H., Evans P. A., Udalski A., 2017, *MNRAS*, 471, 3878
 Trudolyubov S. P., 2008, *MNRAS*, 387, L36
 Tsygankov S. S., Doroshenko V., Lutovinov A. A., Mush-tukov A. A., Poutanen J., 2017, *A&A*, 605, A39
 Trudolyubov S. P., Priedhorsky W. C., Córdova F. A., 2007, *ApJ*, 663, 487
 Vasilopoulos G., Lander, S.K., Koliopanos, F., Bailyn, C.D., 2019, *MNRAS*, in press, arXiv:1911.09670
 Walton D. J., et al., 2018, *ApJ*, 857, L3
 Willems B., Kalogera V., Henninger M., 2004, *ApJ*, 616, 414

APPENDIX A: OBSERVED PROPERTIES OF NSULXS

In this appendix we present a table with the observed properties of all known neutron-star ULX. It is an updated version of Table 1 of King & Lasota (2019).

This paper has been typeset from a \LaTeX file prepared by the author.

Table A1. Observed properties of NSULXs

Name	L_X (max) [erg s $^{-1}$]	P_s [s]	$\dot{\nu}$ [s $^{-2}$]	P_{orb} [d]	M_2 [M_\odot]
M82 ULX2 ¹	2.0×10^{40}	1.37	10^{-10}	2.51 (?)	$\gtrsim 5.2$
NGC7793 P13 ²	5×10^{39}	0.42	2×10^{-10}	63.9	18–23 (B9I)
NGC5907 ULX1 ³	$\sim 10^{41}$	1.13	3.8×10^{-9}	5.3(?)	
NGC300 ULX1 ^{4,5}	4.7×10^{39}	~ 31.5	5.6×10^{-10}		8 - 10 (?) (RSB)
M51 ULX-7 ^{6,7}	7×10^{39}	2.8	2.8×10^{-10} (3.1×10^{-11})	~ 2	> 8
SMC X-3 ^{8,9}	2.5×10^{39}	~ 7.7	6.9×10^{-11}	45.04	> 3.7 (Be ?)
NGC 2403 ULX ¹⁰	1.2×10^{39}	~ 18	3.4×10^{-10}	60 – 100 (?)	(Be ?)
Swift J0243.6+6124 ¹¹	$\gtrsim 1.5 \times 10^{39}$ (?)	9.86	$2.2. \times 10^{-10}$	28.3	(Be ?)
NGC 1313 PULX ¹²	1.6×10^{39}	~ 765.6			(Be ?)
M51 ULX8 ¹³	2×10^{39}	NO	NO	8 – 400 (?)	40 (?)

¹Bachetti et al. (2014), ²Fürst et al. (2016); Fürst, et al. (2018); Israel et al. (2017a); Motch et al. (2014); ,³Israel et al. (2017b) ⁴Carpano et al. (2018), ⁵Heida, et al. (2019b), ⁶Rodríguez Castillo, et al. (2019), ⁷Vasilopoulos et al. (2019),⁸Trudolyubov, Priedhorsky, & Córdova (2007); ⁹Doroshenko, Tsygankov, & Santangelo (2018), ¹⁰Tsygankov et al. (2017), ¹¹Townsend et al. (2017), ¹²Trudolyubov (2008), ¹³Brightman et al. (2018).